INTERNATIONAL JOURNAL OF INTEGRATED ENGINEERING
ISSN: 2229-838X e-ISSN: 2600-7916

IJIE

Vol. 17 No. 1 (2025) 353-366
https://publisher.uthm.edu.my/ojs/index.php/ijie

Advanced Heat Sink Integration Strategies for Monocrystalline Solar Panel Performance Enhancement

M. Akmal Ma'arif[1], Levin Halim[1]*, Christian Fredy Naa[1]

[1] *Jl. Cieumbuleuit No. 94, Bandung, Department of Electrical Engineering, Parahyangan Catholic University, 40141, INDONESIA*

*Corresponding Author: halimlevin@unpar.ac.id
DOI: https://doi.org/10.30880/ijie.2025.17.01.029

Article Info

Received: 4 August 2024
Accepted: 2 November 2024
Available online: 30 April 2025

Keywords

Radiation, heat sink, solar panels, temperature

Abstract

Renewable energy is an alternative solution to solve the problem of global warming. One of the ways to help these problems is to take advantage of solar energy. Solar panels are tools that can transform solar energy into electrical energy. However, solar panels have efficiency sensitivity. In several previous studies, heat sinks can increase the efficiency of solar panels. Therefore, this research is conducted to determine the increase in the efficiency of monocrystalline solar panels using a heat sink. This study uses solar panels of monocrystalline type with the MS50M-18 series. Data collection is carried out with a data logger system using a digital multimeter and Arduino as the direct way, taking at most 140 data every 15 seconds. This study concludes that there is an increased efficiency of solar panels using a heat sink from 8.8% to 11.89% on radiation 700 W/m2 where the maximum temperature is from 77 ◦C to 72 ◦C when using a heat sink. These findings demonstrate the effectiveness of passive cooling using heat sinks, contributing to optimizing solar panel performance in moderate irradiance conditions. The proposed system offers a low-cost and scalable solution for improving solar energy generation in various environmental settings.

1. Introduction

Renewable energy resources have been a focal point of intensive research in addressing climate change caused by exploiting conventional energy sources [1]. Renewable energy, particularly solar energy, is considered a solution to the escalating global energy consumption [2]. However, one of the challenges in solar energy development is the relatively low efficiency of solar panels [3–5]. On the other hand, there is an issue with the solar panel's temperature, which shows that an increase in temperature on solar cells can decrease voltage due to the excitation of electrons from higher energy levels compared to the energy of the semiconductor material [6–8].

Nomenclature

I_{pv}	Output current from solar cells (A)	ϵ	*Effectiveness Heat Sink*
I_{ph}	Current Which grow consequence broadcasting photon (A)	ϕ	*Ratio areas fin*
I_d	Current Which pass diode (A)	H	*Heat Transfer coefficients (Base / Fin) (W/m ^{2} .K)*
I_{sh}	Current Which pass obstacle *shunt* (A)	H	*Heat Transfer coefficients (Surface* / Fin) (W/m ^{2} .K)
I_s	Current saturation diode (A)	S	*Dimensional parameters*
m	farctor ideal diode	D	*Dimensional parameters*
q	Payload Diode (C)	Bi	*Biot Numbers* (K)
σ	Constant Boltzmann (1.38x10 $^{-23}$ JK $^{-1}$)	T_∞	Temperature environment (K)
T	Temperature (K)	P''_e	Power Dissipated (W/m ^{2})
R_s	Barriers on cell Sun (R)	P''_e	Thermal Resistance (m ^{2} .K/W)
V_{pv}	Voltage cell Sun (V)	L	High *heat sink* (m)
V_{diode}	Voltage on diode (V)	h	*Heat Transfer Coefficient* (W/m ^{2} .K)
V_{shunt}	Obstacle on shunt (Ω)		
V_{mp}	Voltage When Power maximum (V)		

The temperature of the solar panel module significantly impacts the voltage and current at the electrodes. As illustrated in Fig. 1, an increase in temperature leads to a decrease in both voltage and current, resulting in a reduction in the efficiency of the solar panel due to the temperature-induced decline in the current-voltage relationship. This phenomenon is particularly evident during daylight hours when temperatures rise. The corresponding current-to-voltage curve shows variations with changing radiation levels, highlighting the importance of maintaining a constant temperature during cell operation. Several graphs displaying current-voltage characteristics at different radiation levels are necessary to observe temperature-related variations effectively. For instance, as the temperature reaches its maximum, there is a known reduction of up to 19.5% when increasing the temperature from 20 to 50 degrees Celsius. The voltage at the open circuit linearly decreases with rising temperature. Temperature variations commonly affect short circuits at a rate of +0.5% per degree Celsius, and an increase in temperature leads to a reduction in open circuit voltage at a rate of -0.5% [9].

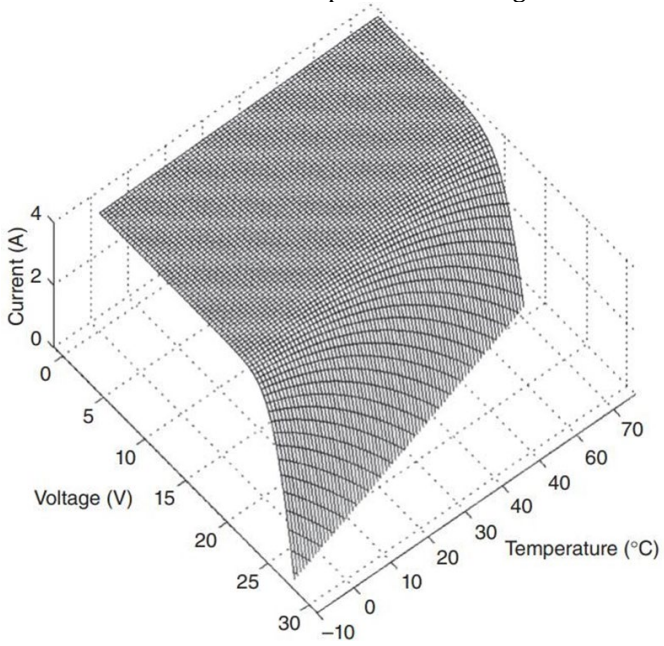

Fig. 1 *Influence voltage, current, and temperature on solar panel [10]*

It is proven that the efficiency of solar cells with silicon crystal structures will decrease by 0.4–0.5% for a 1°C increase in temperature [11]. Thus, the operational temperature of solar panels becomes an essential parameter to achieve better efficiency for photovoltaic systems [12], hence making the cooling system of the solar panel important.

Several research studies have demonstrated the effectiveness of cooling systems in improving solar panel efficiency. A study showed a temperature reduction of 6.1°C and an increase in power by 1.77% by incorporating a flat aluminum plate (heat sink) behind the solar panel as part of passive cooling [13]. Another research indicated

Int. Journal of Integrated Engineering Vol. 17 No. 1 (2025) p. 353-366

that the efficiency of solar cells could be enhanced by reducing the working temperature, which was achieved by adding cooling fins beneath the panel's surface, resulting in a 1.8% higher solar panel efficiency [14]. Research [15] shows that fin cooling systems for photovoltaic panels produce the highest power generation, while improperly selected Phase Changing Material (PCM) and thermoelectric materials can increase surface temperatures and decrease output power. On the other hand, research [16] proved that dual surface cooling of solar photovoltaic panels using cotton wick mesh significantly improves electrical efficiency and energy yield, reducing the temperature by 23.55°C. Furthermore, hydrogel beads with fins can effectively cool solar panels, reducing temperature by 10°C and increasing electricity generation efficiency by 7.2% [17].

Although there have been advances in solar panel cooling technologies, solar cells still experience efficiency limitations due to high operating temperatures. One of the cooling systems for solar panels, passive cooling techniques, such as heat sinks, has demonstrated their potential to increase efficiency. However, while active cooling solutions exist, they typically cost more and are not practical, especially in off-grid photovoltaic systems.

This research objective is to achieve increased efficiency by implementing a cooling system that utilizes heat sinks on solar panels. The effectiveness of using heat sinks as a passive cooling system to improve the efficiency of monocrystalline solar panels by reducing their operating temperature will be evaluated. Specifically, the research aims to quantify the impact of different radiation levels on the panel's performance with and without a heat sink. The goal is to optimize performance and enhance efficiency. This cooling system can potentially boost the power performance of photovoltaic systems.

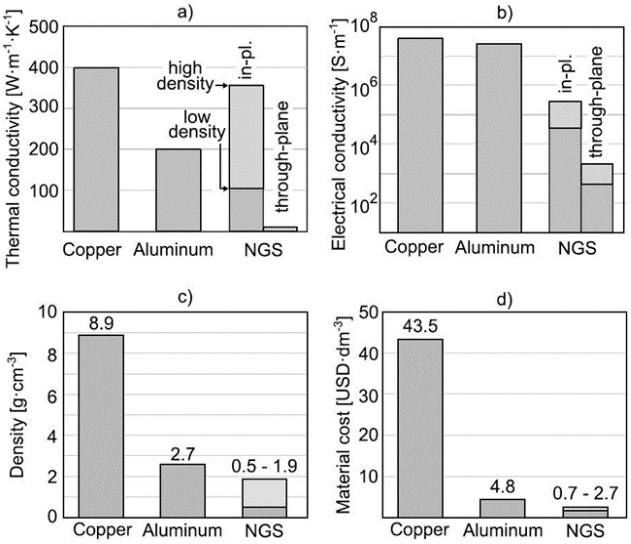

Fig. 2 *Comparison heat sink material [9]*

In this study, the cooling system component utilized heat sinks. The material used for the heat sink component typically consists of unique materials, with copper or aluminum commonly employed due to their favorable thermal conductivity values, which further details can be found in Fig. 2 [9].

This research is limited to investigating monocrystalline solar panels with heat sinks under laboratory-controlled conditions using a sun-substitute kit. To simulate high, medium, and low sunlight exposure, the study focuses on three specific radiation levels (1300 W/m^2, 700 W/m^2, and 300 W/m^2). The scope excludes active cooling methods and focuses on passive cooling using aluminum heat sinks.

The research employs a laboratory-scale experimental setup, where monocrystalline solar panels (MS50M-18) are subjected to radiation from halogen lamps to simulate sunlight. A heat sink is attached to the rear of the solar panels to dissipate heat. Temperature data is collected using thermocouples connected to an Arduino system, while voltage and current data are recorded using a digital multimeter. The study analyzes the panels' efficiency by comparing performance metrics under different radiation levels, with and without the heat sink. The experimentation was conducted on a laboratory scale using a setup that substitutes sunlight with a 20-watt halogen lamp, consisting of 40 lights generating radiation equivalent to 1300 W/m^2. In this study, the solar panel is monocrystalline, which uses a heat sink with 12 fins for the cooling system. After the experimental setup, data was collected to obtain temperature readings from solar panels without and with a heat sink. The obtained data

were processed to represent the characteristics of a solar panel: V-I Curve and V-P Curve. The characteristics of the solar panel are then analyzed by comparing the results with and without a cooling system.

2. Methodology

The methodology is designed to observe the effectiveness of a heat sink cooling system on monocrystalline to decrease the solar panel's temperatureThe process involves setting up a sun-substitute kit, attaching a cooling system, collecting data using a digital multimeter and thermocouple sensors, and analyzing the performance metrics at several various solar radiation levels.

2.1 Sun-Substitute Kit

For the sun-substitute kit, a table is shaped to resemble a table with a frame attached at the top to accommodate halogen lamps. The lamps and dimmer are connected with a white twin cable with a voltage of AC 220 Volts. The table measures 63 cm in length, 40 cm in width, and 60 cm in height. The position of the lamps is separated from the table to facilitate researchers in adjusting the distance between the panel and the lamps. The halogen lamps are arranged in 10 rows with a 6 cm distance between each lamp, with each row containing four lamps connected to sockets. This distance is intended to enhance the effectiveness of the halogen lamp radiation distribution. The sun-substitute kit for the experimental study for this research is shown in Fig. 3.

Fig. 3 *Sun-substitute kit*

2.2 Cooling System for Solar Panel

A heat sink is placed on the rear side of the solar panel, where it can dissipate heat from the radiation received from the solar cells. The heat sink and the solar panel are the locations for three thermocouple sensors for collecting temperature data. These sensors are positioned on the solar panel, the heat sink base, and the fins' top. Fig. 4 shows the solar panel's backside with the installed heat sink.

Int. Journal of Integrated Engineering Vol. 17 No. 1 (2025) p. 353-366

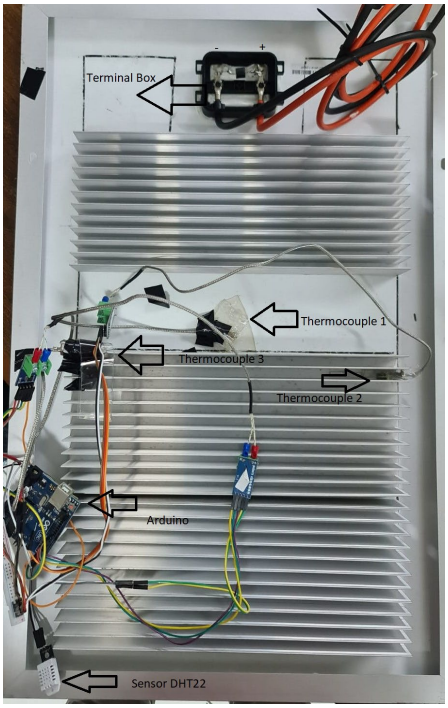

Fig. 4 *The back side of the solar panel with the installed heat sink*

As shown in Fig. 4, a terminal box on the rear side of the solar panel serves as the output source connected to a clamp cable leading to a digital multimeter. There are three heat sinks strategically positioned with specific gaps to facilitate the effective dispersion of the cooling system on the back side of the solar panel. The distances between the three heat sinks are set to optimize the cooling system. In the middle of the solar panel, there is an 8 cm gap to allow contact with thermocouple sensor 1, ensuring a 5 cm distance from the adjacent heat sink. Thermocouple sensors 2 and 3 are affixed to the base and top fins of the heat sink, respectively. These sensors are placed to monitor temperatures on the heat sink's base and upper fin attached to the second heat sink, as shown in Fig. 4. This arrangement is designed to capture temperatures at the midpoint of the solar panel, where the highest temperatures are recorded. The placement of these heat sinks effectively forms a cooling system for the solar panel, reducing high temperatures.

2.3 Data Collection Method

The data collection in this research involves using a data logger system, where data is acquired directly within specific time intervals. The data used in this research include the temperature of the lower part of the panel, ambient temperature, output voltage, and current values. The data is obtained in real-time with a period of 15 seconds and varies in quantity for each radiation level: 100 data points for 1300 W/m^2, 140 data points for 700 W/m2, and 60 data points for 300 W/m^2. The discrepancy in data quantity is due to considering the maximum regulation reached by each radiation level as the temperature stabilizes at the maximum point. The data logger system utilizes a microcontroller and a digital multimeter connected to a laptop via a data cable.

On the other hand, the halogen lamp intensity is controlled with dimmers to achieve the desired solar radiation level. Three radiation levels are considered in this research: 1300 W/m^2, 700 W/m^2, and 300 W/m^2. The dimmer settings are adjusted to achieve 100% radiation for 1300 W/m^2, 70-65% for 700 W/m^2, and 40-30% for 300 W/m^2.

This research selected the 1300 W/m^2 level to represent high solar radiation levels, typically during peak daylight hours, representing the upper limit of natural solar radiation level, as shown in [2,3]. On the other hand, the 700 W/m^2 solar radiation level was chosen to represent moderate solar conditions during mornings, afternoons, or areas with partial clouds [18]. Lastly, the 300 W/m^2 solar radiation level typically occurs during early mornings, late afternoons, or under overcast skies. This variation of solar radiation level is to evaluate the cooling system's performance at various levels of solar radiation [11]. These three solar radiation levels will provide a more comprehensive analysis of the impact of heat sinks on solar panel efficiency at different solar radiation levels. So, it will provide practical insight into its potential application in the real world.

The data collection is conducted utilizing the electrical circuit as shown in Fig. 5. An Arduino microcontroller UNO is used as a component to assist in gathering data from four temperature sensors, including a thermocouple and DHT22. The data is acquired using the PLX-DAQ application, which transfers data read by the sensors through

Arduino with a delay time (in seconds) determined by the code in Arduino, customized to accommodate the radiation conditions. A digital multimeter (Rigol DMM3058) retrieves solar panel voltage and current data. The data is obtained through the Jupyter application connected to the device, with data retrieval occurring at specific time intervals and quantities set in the Jupyter code. Once the data is retrieved, it is automatically saved in (.csv) format for easy input into Excel for further processing.

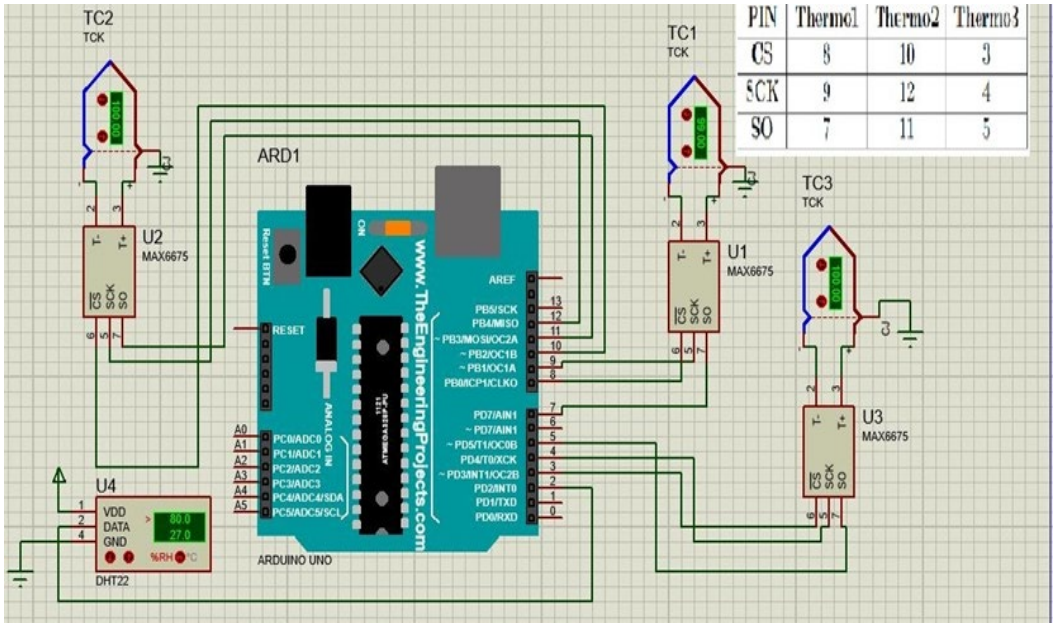

Fig. 5 *Temperature data collection electrical circuit*

The data acquisition method consists of the following steps, as shown in the flowchart in Fig. 6:

1. The first step is to prepare all necessary equipment for data acquisition, including connecting the digital multimeter and thermocouple sensors to an Arduino system linked to a laptop using a data cable B. Ensuring that all devices are correctly connected and calibrated before proceeding is crucial.
2. A decision point occurs here, asking, "Are all devices connected and calibrated correctly?" If the answer is No, the devices must be checked and reconnected. If the answer is Yes, the process continues to the next step.
3. After verifying device connections, the halogen lamp in the solar replacement kit is turned on. The brightness is adjusted using a dimmer to achieve the desired radiation level. This is done while monitoring the radiation value using a solar power meter.
4. Another decision point asks, "Is the desired radiation level achieved?" If the answer is No, further adjustments are made to the halogen lamp brightness using the dimmer. If the answer is Yes, the process proceeds to the next step.
5. Once the radiation level is set, the code is configured in the Jupyter application to determine the amount of data to be collected and the delay per data point. Data acquisition begins based on these parameters.
6. Another decision point arises during the data collection process: "Has the temperature stabilized at the maximum point?" If No, data collection continues until the temperature stabilizes. Once stabilization is confirmed (Yes), the process moves forward.
7. Once the temperature stabilizes and sufficient data is collected, the system stores the data and stops the data acquisition process.
8. After verifying that data collection is complete, the final step is to disconnect the PLX-DAQ device and all other equipment.

Int. Journal of Integrated Engineering Vol. 17 No. 1 (2025) p. 353-366

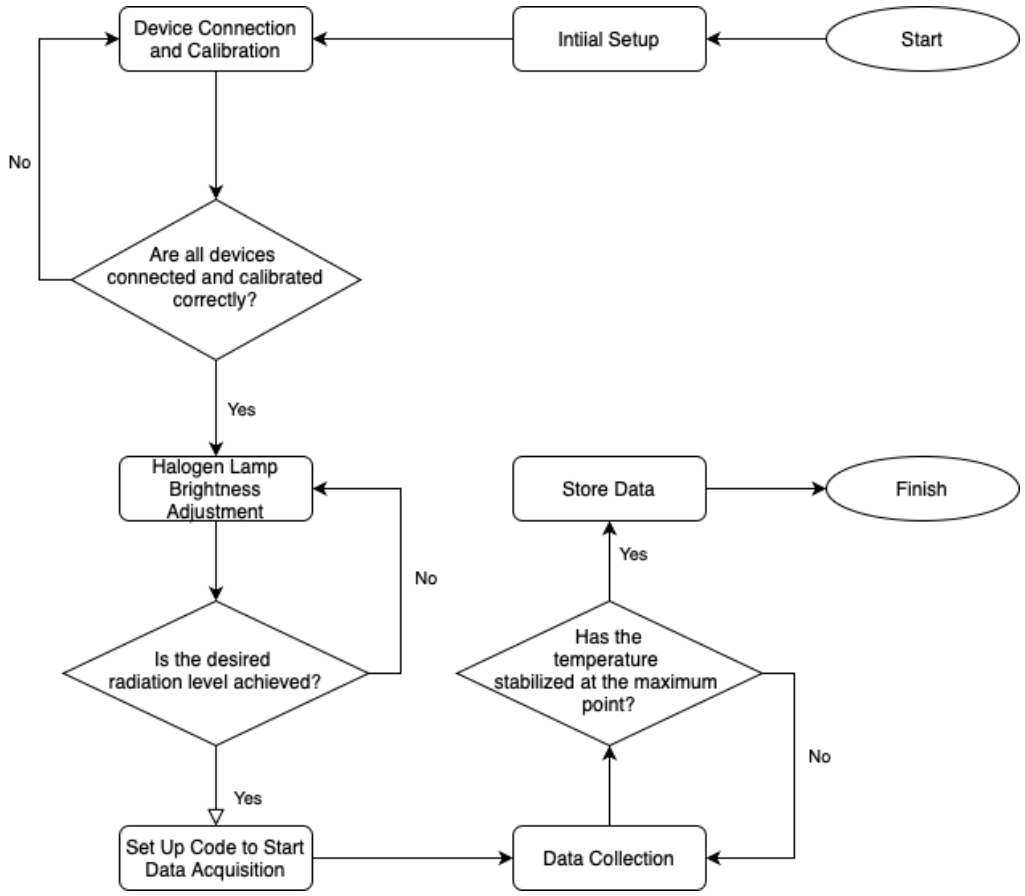

Fig. 6 *Flowchart of data acquisition method*

For the solar panel characteristics data collection, the processed data is presented in characteristic charts obtained from the initial temperature of 25°C and the maximum temperature (steady state) under each radiation condition. Each radiation condition produces a distinct characteristic graph due to differences in voltage and current values obtained. Variations in resistance (Ω) are essential in collecting characteristic data to form a graph illustrating the solar panel's characteristics. Each resistance value generates data on different voltage and current values for the circuit. The circuit diagram shows the configuration for obtaining voltage and current data characterizing the solar panel. The solar panel characteristics data collection circuit is shown in Fig. 7.

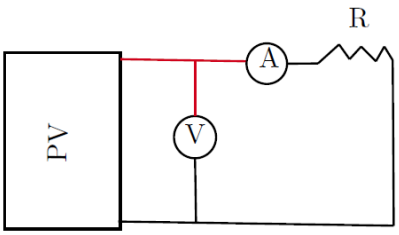

Fig. 7 *Solar panel characteristics data collection circuit*

The red line represents the power source (+) from the solar panel, while the black line indicates the ground (-). The symbol A denotes the point for collecting current data, and V is the location for obtaining voltage data. This method involves using two digital multimeters to capture voltage and current values. Additionally, the symbol R represents the variable resistor with nine different values, adjusted during each data collection session using a crocodile cable to facilitate easy resistance variation.

3. Results and Discussion

In this section, the performance of monocrystalline solar panels with and without the use of a heat sink is analyzed. The results are presented by comparing the voltage, current, and temperature data under three different radiation

levels: 1300 W/m^2, 700 W/m^2, and 300 W/m^2. This analysis highlights the effectiveness of the passive cooling system in enhancing solar panel efficiency.

3.1 Solar Panel

Solar panels are devices capable of converting solar energy into electrical energy; however, a limitation lies in the relatively small efficiency of these solar panels [4]. The electric voltage generated by a solar cell is relatively small, approximately 0.6 V without any obstacles and 0.45 V with obstacles. Several solar cells arranged in series are required to achieve a higher electrical voltage, resulting in a 16 V. This voltage proves sufficient to supply a 12 V battery. The combination of multiple solar cells is called a solar panel or module. Arranging around 10 to 20 or more solar panels can yield high current and voltage suitable for daily energy needs [19]. It's worth noting that various types of solar panels exist, including Monocrystalline, Polycrystalline, and Thin PV Film [20]. This research employed Monocrystalline solar panels, specifically the MS50M-18 series, which has a power output of 50 Wp. This type was chosen due to its easy availability in the market, capacity to generate significant power output, and ease of data retrieval. This selection facilitates the practical aspects of the research while ensuring reliable and relevant data acquisition. The solar panel utilized for the study is shown in Fig. 8. The Monocrystalline Solar Panel Type MS50M-18 specification is shown in Table 1.

Fig. 8 *Monocrystalline solar panel type MS50M-18*

Table 1 *Specification monocrystalline solar panel*

Specification	
Type	MS50M-18
Dimension (mm)	400 × 625 × 25
Voc	22.1 V
Isc	2.94 A
Imp	2.78 A
Vmp	18 V

The efficiency value is crucial to determine the output value of this research. To obtain this value, it is necessary first to calculate the fill factor using the fill factor equation, which plays a crucial role in determining the dimensions of a solar panel. The fill factor equation is presented in equation (1) [21].

$$FF = \frac{V_{mp} I_{mp}}{V_{oc} I_{sc}} = \frac{50.04}{64.97} = 0.77 \quad (1)$$

Efficiency refers to the output generated by a power source about the maximum possible input, signifying the system's effectiveness in utilizing the available power source. The higher the system's efficiency, the more adept it is at extracting energy from the power source. Efficiency can be represented in an equation, as indicated by equation (2) [22].

Int. Journal of Integrated Engineering Vol. 17 No. 1 (2025) p. 353-366

$$\eta_{sp} = \frac{V_{oc} \times I_{sc} \times FF}{SI \times A} \times 100\% = \frac{22.1 \times 2.97 \times 0.77}{1000 \times 0.4 \times 0.625} = 20\% \quad (2)$$

3.2 Heat Sink

A heat sink is a component primarily designed for cooling specific elements. Typically, heat sinks are made of aluminum or copper, which are recognized for their effective heat dissipation properties. They are commonly utilized as part of a computer's CPU components. The heat sink is designed to absorb the heat emitted by the device and transfer it to a fluid medium [23]. Table 2 shows the specifications of the heat sink.

Table 2 *Specification of heat sink*

Specification	
Material	Aluminium
Dimension (mm)	50 × 30 × 3
Amount Fin	12 fin
Thick Base	0.0036 m
Fin Thickness	0.002 m

Based on Table 2, attention is directed to one specific fin on the heat sink to determine the fin model of a heat sink. The theory suggests that the heat received at the heat sink's base is then transferred to the fins, allowing heat dissipation using the ambient temperature. The model employed aims to establish the temperature dissipated by the heat sink fins, as illustrated in Fig. 4.

3.3 Data Comparison Analysis

The analysis obtained from this research can be explained through a comparison of graphs illustrating the characteristics of the solar panel. This comparison considers the performance of the solar panel when using a cooler compared to not using a cooler, particularly in terms of temperature variations, as well as changes in voltage and current generated by the solar panel under three different radiation levels: 1300 W/m^2, 700 W/m^2, and 300 W/m^2. The following is an analysis of the obtained comparative data.

The V-I characteristic graph shows the performance of the solar panel used. When the solar panel is cooled, the temperature decreases, increasing the output current and voltage compared to not using a cooler. Characteristics can be observed through obtained data to assess the solar panel's performance, including open-circuit voltage, short-circuit current, output voltage, and current data connected with variations in resistance to observe characteristic graphs. As shown in the graphs in the solar panel characteristic study, the panel receives three types of radiation, namely 1300 W/m^2, 700 W/m^2, and 300 W/m^2. For radiations of 1300 W/m^2 and 300 W/m^2, the characteristics of the solar panel do not undergo significant changes when using a cooler. At the maximum temperature produced under 1300 W/m^2 radiation, there is a reduction in the maximum temperature from 95°C to 89°C. However, the characteristic graph has no significant change compared to the cooling method.

As shown in the V-I Characteristics at Initial Temperature in Fig. 9, for the solar radiation of 700 W/m^2, the V-I characteristic indicates that there is a significant change when using a cooler. It can be said that at this radiation level, the effectiveness of the cooler's impact on the solar panel becomes apparent. Under 700 W/m^2 radiation, the maximum temperature is 77°C without a cooler and 72°C with a cooler. With this change, it is theorized that this radiation level can increase the output voltage and current generated by the solar panel. When the temperature reaches its maximum (steady state), the V-I characteristics change compared to the initial temperature (25°C). At maximum temperature, the output voltage and current values are compared using the cooling method and not the cooling method.

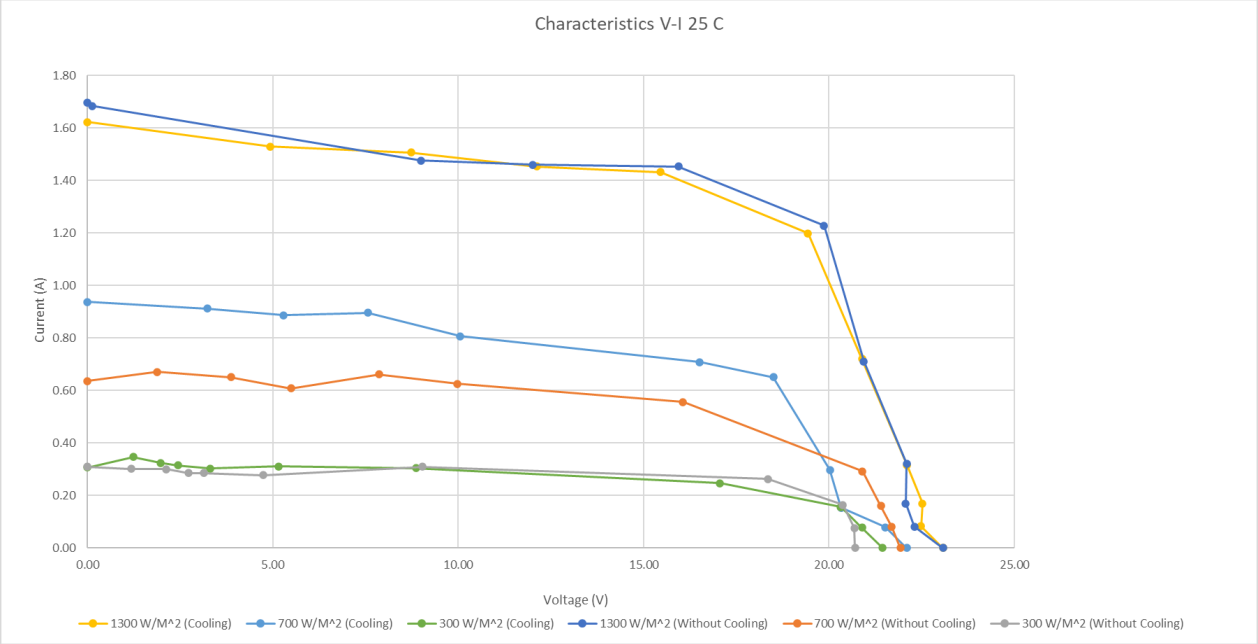

Fig. 9 *V-I characteristics at initial temperature (25°C)*

The characteristics of V-I at Maximum Temperature are shown in Fig. 10. The solar panel reaches its maximum temperature, and there is a difference in temperature values among the three radiations when using a cooler and not using a cooler. The V-I characteristic of the solar panel at maximum temperature (steady state) explains that using the cooling system impacts the increase in voltage and current values on the solar panel. The voltage and recent value changes are significant under 700 W/m² radiation, showing a more notable difference compared to 1300 W/m² and 300 W/m² radiations.

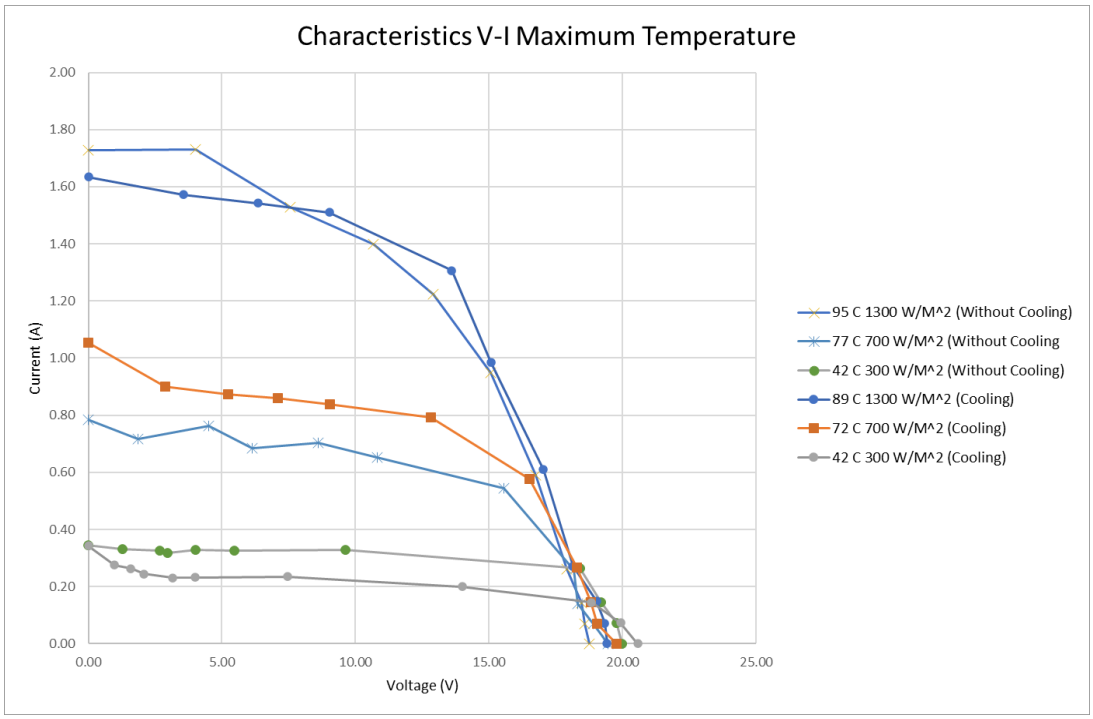

Fig. 10 *V-I characteristics at maximum temperature (Steady state)*

Int. Journal of Integrated Engineering Vol. 17 No. 1 (2025) p. 353-366

The comparison graph of V-P characteristics illustrates the power generated by the solar panel when using the cooling method and when not using the cooling method at the initial temperature (25°C). For a clearer view, it is shown in the V-P characteristic graph at a temperature of 25°C.

On the other hand, the V-P Characteristics at the initial temperature are shown in Fig. 11. It is shown that after using the cooling system component, the heat sink, there is a significant change in the power generated, particularly under the 700 W/m^2 radiation. Previously, in the V-I characteristic graph (Fig. 9), changes occurred in this radiation due to alterations in the output voltage, current, and power produced. When the temperature reaches its maximum (steady state), there is a change in the generated power compared to the initial temperature (25°C).

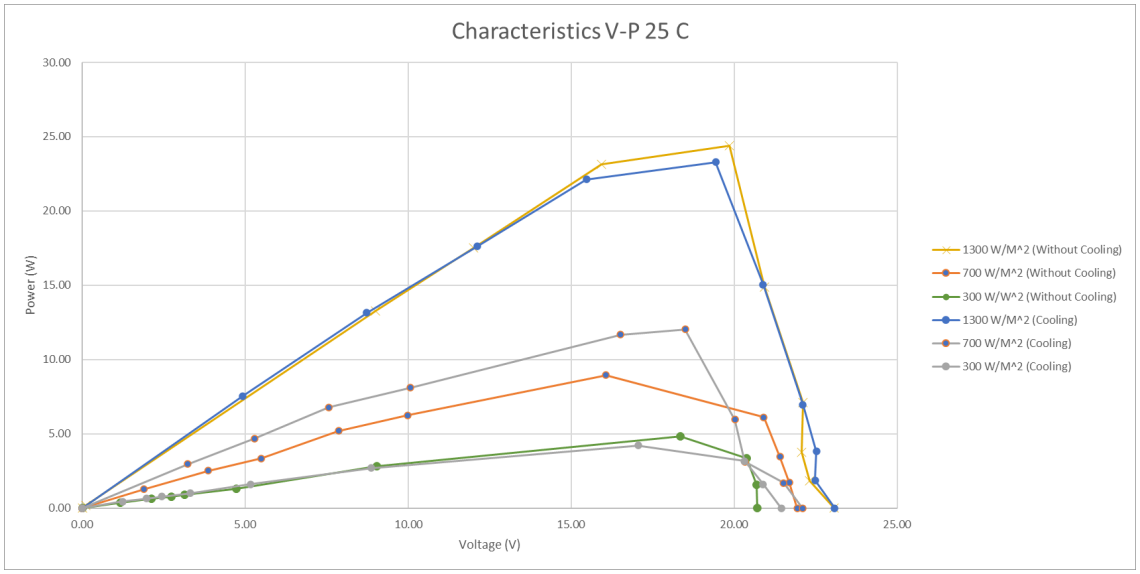

Fig. 11 *V-P characteristics at initial temperature (25°C)*

Fig. 12 is similar to the V-I characteristics at maximum temperature (steady state), the V-P characteristics at maximum temperature (constant state) change the generated power when compared to a using cooler and not using a cooler. Under 700 W/m^2 radiation, there is a significant change in power values compared to 1300 W/m^2 and 300 W/m^2 radiation.

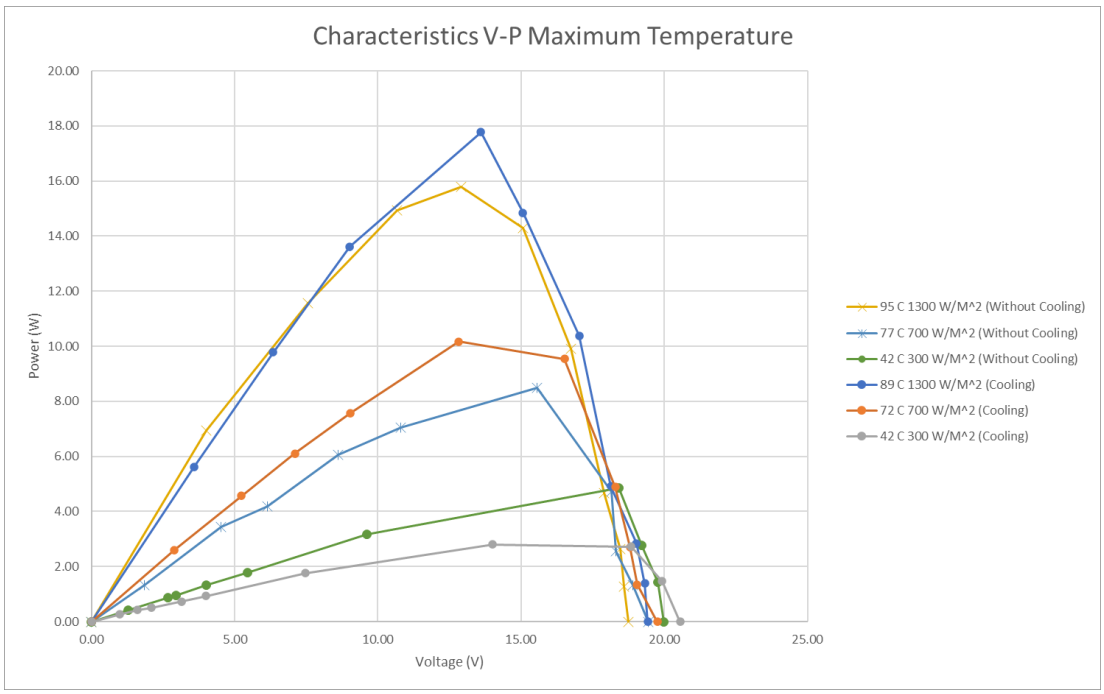

Fig. 12 *Graph of V-P characteristics at maximum temperature (Steady state)*

The substantial increase in efficiency observed at 700 W/m^2 radiation indicates that passive cooling methods, such as the heat sink, can effectively optimize solar panel performance. However, in high solar radiation environments (with consistent sunlight close to 1300 W/m^2), while the efficiency improvements are less significant, the cooling system still plays a crucial role in improving the solar panel's efficiency by preventing overheating. This can reduce the risk of long-term thermal degradation, extending the lifespan of photovoltaic systems in harsh conditions.

Moreover, the passive nature of the cooling system makes it highly suitable for deployment in off-grid solar systems, where maintenance and energy efficiency are critical. By reducing the need for active cooling (which would consume additional power), this solution provides a cost-effective method for enhancing the energy output of solar panels, particularly in rural or isolated areas where energy resources are limited. This scalability and ease of implementation make the proposed cooling system attractive for small and large-scale solar installations.

3.4 Improvement of Solar Panel Efficiency

Evaluating the effectiveness of this study involves incorporating the output voltage and current variables obtained. The efficiency and fill factor equations are expressed in Equations 1 and 2, respectively, utilizing variables derived from the data collected in this investigation. The efficiency values for the three radiations, 1300 W/m^2, 700 W/m^2, and 300 W/m^2, at the initial temperature (25°C), which is shown in Table 3.

Table 3 *Solar panel efficiency on initial temperature (25°C)*

Radiation	Without Heat Sink		Use Heat Sink	
	Fill Factor	Efficiency	Fill Factor	Efficiency
1300 W/m ^{2}	1,005	12.1%	1,011	12.7%
700 W/m ^{2}	1.02	8.1%	1,003	11.9%
300 W/m ^{2}	1.01	8.6%	1.10	9.74%

The efficiency at the initial temperature significantly increases compared to operating without cooling, making a noticeable difference. These variations are particularly apparent in the case of 700 W/m^2 radiation, where the efficiency improvement is more pronounced than other radiations, where changes are less conspicuous. At the maximum temperature (steady state), observed at 1300 W/m^2 radiation, the maximum temperature reaches 95°C. For 700 W/m^2 radiation, the maximum temperature is 77°C; for 300 W/m^2 radiation, the maximum temperature is 42°C. After a cooling method is utilized, the solar panel results in reduced maximum temperatures of 89°C, 72°C, and 42°C, respectively.

Based on the solar panel's efficiency at the maximum temperature shown in Table 4, the efficiency value at the maximum temperature remains relatively consistent compared to the initial temperature. However, in the case of 700 W/m^2 radiation, there is a noteworthy and significant change, making it an effective radiation in this study. This change indicates an enhancement in efficiency compared to other radiations.

Table 4 Solar panel efficiency on temperature maximum (Steady state)

Radiation	Without Heat Sink		Use Heat Sink	
	Fill Factor	Efficiency	Fill Factor	Efficiency
1300 W/m ^{2}	1.005	10%	1.011	10.2%
700 W/m ^{2}	1.02	8.8%	1,003	11.89%
300 W/m ^{2}	1.01	9%	1.10	10%

4. Conclusion

This study delves into the effectiveness of a passive cooling system employing aluminum fins on Sun MS50M-18 monocrystalline solar panels. It aims to understand how temperature variations impact solar panel efficiency, mainly focusing on the role of the cooling system in reducing temperature-induced performance degradation. The research reveals that the cooling system significantly mitigates the rise in maximum panel temperatures, particularly noteworthy under 700 W/m^2 radiation conditions, where substantial improvements in voltage, current output, and overall efficiency are noted. Data collection methodologies encompass a comprehensive approach, utilizing digital multimeters and thermocouple temperature sensors integrated with Arduino for direct data acquisition. The results underscore the substantial effectiveness of the cooling system in attenuating the

maximum temperature range experienced by the solar panels, thus enhancing their overall performance and longevity. The practical significance of this research is evident in its potential application to real-world solar panel systems. The passive cooling method using aluminum heat sinks has demonstrated effectiveness in improving solar panel efficiency under a range of irradiance conditions. Given the low cost and ease of implementation, this passive cooling solution is well-suited for off-grid and remote applications, where system efficiency and reliability are crucial. Future research could explore different heat sink materials, such as copper, and alternative fin designs to improve cooling efficiency. Testing the system in various environmental conditions, such as humid or cold climates, would also provide insights into its performance in different locations.

Acknowledgement

The authors acknowledge the support from Parahyangan Catholic University throughout this project.

Conflict of Interest

The authors declare no conflict of interest regarding the paper's publication.

Author Contribution

The authors confirm their contribution to the paper as follows: ***study conception and design:*** *M. Akmal Ma'arif, Christian Fredy Naa;* ***data collection:*** *M. Akmal Ma'arif;* ***analysis and interpretation of results:*** *M. Akmal Ma'arif, Levin Halim;* ***draft manuscript preparation:*** *M. Akmal Ma'arif, Levin Halim. All authors reviewed the results and approved the final version of the manuscript.*

References

[1] Halkos, G.E. and Gkampoura, E.-C. (2020). Reviewing Usage, Potentials, and Limitations of Renewable Energy Sources, *Energies*, 13(11), 2906, https://doi.org/10.3390/en13112906
[2] Arifin, Z., Tjahjana, D.D.D.P., Hadi, S., Rachmanto, R.A., Setyohandoko, G. and Sutanto, B. (2020). Numerical and Experimental Investigation of Air Cooling for Photovoltaic Panels Using Aluminum Heat Sinks, *International Journal of Photoenergy*, 2020, 1–9, https://doi.org/10.1155/2020/1574274
[3] Wang, Y., Liu, H. and Zhu, J. (2019). Solar thermophotovoltaics: Progress, challenges, and opportunities, *APL Materials*, 7(8), https://doi.org/10.1063/1.5114829
[4] Laurensia, M. and Halim, L. (2024). Optimizing solar panel efficiency utilizing reflectors and water treatment techniques, *Journal of Energy Systems*, 8(2), 116–29, https://doi.org/10.30521/jes.1352390
[5] Al-Shahri, O.A., Ismail, F.B., Hannan, M.A., Lipu, M.S.H., Al-Shetwi, A.Q., Begum, R.A. et al. (2021). Solar photovoltaic energy optimization methods, challenges and issues: A comprehensive review, *Journal of Cleaner Production*, 284, 125465, https://doi.org/10.1016/j.jclepro.2020.125465
[6] Libra, M., Petrik, T., Poulek, V., Tyukhov, I.I. and Kourim, P. (2021). Changes in the Efficiency of Photovoltaic Energy Conversion in Temperature Range With Extreme Limits, *IEEE Journal of Photovoltaics*, 11(6), 1479–84, https://doi.org/10.1109/JPHOTOV.2021.3108484
[7] Peng, Z.-W., Buck, T., Koduvelikulathu, L.J., Mihailetchi, V.D. and Kopecek, R. (2019). Industrial Screen-Printed PERT-RJ Solar Cells: Efficiencies Beyond 22% and Open-Circuit Voltages Approaching 700 mV, *IEEE Journal of Photovoltaics*, 9(5), 1166–74, https://doi.org/10.1109/JPHOTOV.2019.2919117
[8] Heo, S., Kim, D.H., Song, Y.M. and Lee, G.J. (2022). Determining the Effectiveness of Radiative Cooler-Integrated Solar Cells, *Advanced Energy Materials*, 12(10), https://doi.org/10.1002/aenm.202103258
[9] Cengel, Y.A. (1997 Jan). Heat Transfer A Practical Approach,
[10] Keyhani, A. (2019). Design of Smart Power Grid Renewable Energy Systems, John Wiley & Sons, Inc., https://doi.org/10.1002/9781119573265
[11] Sachenko, A., Kostylyov, V., Sokolovskyi, I. and Evstigneev, M. (2020). Effect of Temperature on Limit Photoconversion Efficiency in Silicon Solar Cells, *IEEE Journal of Photovoltaics*, 10(1), 63–9, https://doi.org/10.1109/JPHOTOV.2019.2949418
[12] Engelbrecht, D.A. and Tiedje, T. (2021). Temperature and Intensity Dependence of the Limiting Efficiency of Silicon Solar Cells, *IEEE Journal of Photovoltaics*, 11(1), 73–84, https://doi.org/10.1109/JPHOTOV.2020.3035115
[13] Arifin, Z., Suyitno, S., Tjahjana, D.D.D.P., Juwana, W.E., Putra, M.R.A. and Prabowo, A.R. (2020). The Effect of Heat Sink Properties on Solar Cell Cooling Systems, *Applied Sciences*, 10(21), 7919, https://doi.org/10.3390/app10217919
[14] Chen, H., Chen, X., Li, S. and Ding, H. (2014). Comparative study on the performance improvement of photovoltaic panel with passive cooling under natural ventilation, *International Journal of Smart Grid and Clean Energy*, 3(4), 374–9, https://doi.org/10.12720/sgce.3.4.374-379

[15] Bayrak, F., Oztop, H.F. and Selimefendigil, F. (2020). Experimental study for the application of different cooling techniques in photovoltaic (PV) panels, *Energy Conversion and Management*, 212, 112789, https://doi.org/10.1016/j.enconman.2020.112789
[16] Agyekum, E.B., PraveenKumar, S., Alwan, N.T., Velkin, V.I. and Shcheklein, S.E. (2021). Effect of dual surface cooling of solar photovoltaic panel on the efficiency of the module: experimental investigation, *Heliyon*, 7(9), https://doi.org/10.1016/j.heliyon.2021.e07920
[17] Abdo, S., Saidani-Scott, H., Benedi, J. and Abdelrahman, M.A. (2020). Hydrogels beads for cooling solar panels: Experimental study, *Renewable Energy*, 153, 777–86, https://doi.org/10.1016/j.renene.2020.02.057
[18] Zaręba, A., Krzemińska, A., Kozik, R., Adynkiewicz-Piragas, M. and Kristiánová, K. (2022). Passive and Active Solar Systems in Eco-Architecture and Eco-Urban Planning, *Applied Sciences*, 12(6), 3095, https://doi.org/10.3390/app12063095
[19] Kulasekaran, P.S. and Dasarathan, S. (2023). Design and Analysis of Interleaved High-Gain Bi-Directional DC–DC Converter for Microgrid Application Integrated with Photovoltaic Systems, *Energies*, 16(13), 5135, https://doi.org/10.3390/en16135135
[20] Dallaev, R., Pisarenko, T., Papež, N. and Holcman, V. (2023). Overview of the Current State of Flexible Solar Panels and Photovoltaic Materials, *Materials*, 16(17), 5839, https://doi.org/10.3390/ma16175839
[21] [Martini, L., Serenelli, L., Menchini, F., Izzi, M. and Tucci, M. (2020). Silicon heterojunction solar cells toward higher fill factor, *Progress in Photovoltaics: Research and Applications*, 28(4), 307–20, https://doi.org/10.1002/pip.3241
[22] Taruna, C., Halim, L. and Arthaya, B.M. (2019). Initial Concept for Increasing Polycrystalline Fixed Solar Panel Efficiency with Water Treatments, *2019 International Conference on Mechatronics, Robotics and Systems Engineering (MoRSE)*, p. 180–5, https://doi.org/10.1109/MoRSE48060.2019.8998637
[23] Ali, M., Shoukat, A.A., Tariq, H.A., Anwar, M. and Ali, H. (2019). Header Design Optimization of Mini-channel Heat Sinks Using CuO–H2O and Al2O3–H2O Nanofluids for Thermal Management, *Arabian Journal for Science and Engineering*, 44(12), 10327–38, https://doi.org/10.1007/s13369-019-04022-2